rate is $\sim 5 \times 10^{10}$ s^{-1} (Figure 8). This indicates that the reaction falls well within the "normal" region. The plot also includes a data point interpolated from the study by Osuka et al.[7f] involving charge transfer across an aryl-bridged zinc/iron(III) bisporphyrin at a center-to-center separation of 13.6 Å. Although this latter system involves reduction of the central iron(III) ion, rather than the porphyrin ring, k_{ct} correlates well with our data, suggesting similar reorganization energies for the two systems. The structure is such that electron transfer in the aryl-bridged bisporphyrin[7f] should proceed through the spacer, and consequently, it is likely that charge transfer in **4** and **5** also proceeds via a "through-bond" mechanism.

Our results give no information regarding the mechanism of triplet energy transfer although, in view of the relatively large distance, a Dexter mechanism seems appropriate.[37] It is interesting to note the large difference in rates of triplet energy transfer observed for **4** and **5** ($k_{tt}^5/k_{tt}^4 \approx 10$) in view of the almost constant k_{ct} ($k_{ct}^4/k_{ct}^5 \approx 1.3$)[38] over comparable energy gaps. Clearly, the two processes involve quite disparate energy gap dependences, and this finding will be explored further with more appropriate models.

The plateau region in Figure 8 is broad, and k_{ct} remains fairly insensitive to changes in reaction exothermicity over a wide energy range. This behavior, which has been observed for charge-shift reactions involving bimolecular species in frozen media[39] and in model calculations,[40] precludes meaningful determination of the coupling energy between the two porphyrin rings with the present data set. Osuka et al.[7f] found that the rate of reverse electron transfer ($k_{ret} \approx 5 \times 10^8$ s^{-1}) was independent of separation distance and mutual orientation for a range of covalently linked zinc/iron(III) bisporphyrins. For **4**, k_{ret} is 1.7×10^9 s^{-1}, which is a factor of 3 higher than for the zinc/iron(III) bisporphyrin although $\Delta G°$ is ca. −1.2 eV for both systems. The higher rate may be associated with reduction involving the porphyrin ring rather than the metal center.[41] *Furthermore, the same k_{ret} is observed for 4 regardless of the spin multiplicity of the precursor excited state.* This finding is consistent with the high spin–orbital coupling constant of the central gold(III) ion[23] which can affect the apparent spin of the CT state. This being the case, the lifetime of the CT state may be longer than that of a comparable bisporphyrin not possessing a heavy atom.

Acknowledgment. Support for this work was provided by the CNRS and by the Texas Advanced Research Program. The CFKR is supported jointly by the Division of Research Resources of the NIH (Grant RR00886) and by the University of Texas at Austin.

Registry No. **1**, 89372-90-7; **2**, 116123-17-2; **3**, 136316-46-6; **4**, 133724-11-5; **5**, 133724-13-7.

(37) Closs, G. L.; Piotrowiak, P.; MacInnis, J. M.; Fleming, G. R. *J. Am. Chem. Soc.* **1988**, *110*, 2653.

(38) For comparison, k_{ct} values for the following couples were used: k_{ct}^4 refers to **4** with the zinc porphyrin triplet as donor and the gold porphyrin as acceptor and k_{ct}^5 refers to **5** with the gold porphyrin triplet as acceptor and the free-base porphyrin as donor.

(39) Miller, J. R.; Beitz, J. V.; Huddleston, R. K. *J. Am. Chem. Soc.* **1984**, *106*, 5057.

(40) Kakitani, T.; Mataga, N. *J. Phys. Chem.* **1987**, *91*, 6277.

(41) Osuka et al.[7f] comment that the ligand bound to the central iron(III) ion may play an important role in determining the magnitude of k_{ret} but not k_{ct}.

Enhanced Nickel(II) Chelation by *gem*-Dimethyl-Substituted Macrocyclic Tetrathioethers[1]

John M. Desper,[†] Samuel H. Gellman,*[,†] Robert E. Wolf, Jr.,[‡] and Stephen R. Cooper*[,‡]

Contribution from the S. M. McElvain Laboratory of Organic Chemistry, Department of Chemistry, University of Wisconsin, 1101 University Avenue, Madison, Wisconsin 53706, and Inorganic Chemistry Laboratory, University of Oxford, Oxford OX1 3QR, United Kingdom.
Received February 4, 1991

Abstract: The conformational and Ni(II)-binding properties of 1,4,8,11-tetrathiocyclotetradecane (**1**) and derivatives bearing *gem*-dimethyl pairs at the 6- or at the 6- and 13-positions (**2** and **3**, respectively) are compared. The syntheses and crystal structures of **2**, **3**, and their $Ni(ClO_4)_2$ complexes are reported; analogous data for **1** and its $Ni(BF_4)_2$ complex have been in the literature for some time. All three Ni(II) complexes show very similar 14-membered ring conformations, but the metal-free macrocycles display different conformations, in the solid state. These structural data suggest that each *gem*-dimethyl pair progressively biases the macrocycle toward the chelating conformation. We have examined the relative Ni(II) affinities of **1**–**3** in CD_3NO_2 by means of competition experiments monitored by ^1H NMR. Tetrathioether **2** binds Ni(II) approximately 7.3 times more tightly than does **1** at room temperature, and **3** binds Ni(II) approximately 49 times more tightly than does **1**. Thus, each *gem*-dimethyl pair leads to a 1.1 kcal/mol improvement in Ni(II) binding free energy under these conditions. We suggest that the incremental improvement in binding strength across the series **1**–**3** is correlated to the incremental changes in macrocycle conformation observed in the crystal structures of the metal-free thioethers.

Introduction

Ligands that can selectively bind late transition-metal ions are of practical interest because of the ecological and economic significance of these ions. Thioether sulfur is an appealing building block in this regard since it displays a selective affinity for late transition-metal ions relative to other cations.[2] Compared with the vast exploration of the impact of variations in polyether structure on oxophilic cation-binding properties,[3,4] however, relatively little effort has been devoted to examining the effect

[†] University of Wisconsin.
[‡] University of Oxford.

(1) This research was initiated independently in our two laboratories; for preliminary reports, see: (a) Wolf, R. E.; Cooper, S. R. Abstract INOR 173, 185th National Meeting of the American Chemical Society, Seattle, WA, 1983. (b) Desper, J. M.; Gellman, S. H. *J. Am. Chem. Soc.* **1990**, *112*, 6732.

(2) For leading references, see: (a) Cooper, S. R. *Acc. Chem. Res.* **1988**, *21*, 141. (b) Cooper, S. R.; Rawle, S. C. *Structure and Bonding* **1990**, *72*, 1.

(3) Pedersen, C. J. *J. Am. Chem. Soc.* **1967**, *89*, 2495.

0002-7863/91/1513-8663$02.50/0

Table I. Data Collection and Refinement

	2	2 + Ni	3	3 + Ni
mw	296.6	324.6	612.2	681.2
space group	$P2_1/c$	$P\bar{1}$	$P2_1/n$	$P2_1/n$
a, Å	5.468 (2)	5.456 (3)	13.802 (4)	7.535 (5)
b, Å	19.264 (8)	8.943 (3)	12.335 (4)	12.179 (7)
c, Å	14.429 (6)	9.378 (4)	15.472 (5)	14.587 (6)
α		82.30 (3)		
β	99.08 (3)	77.22 (3)	112.25 (2)	93.69 (5)
γ		74.77 (3)		
vol, Å^3	1501.4 (11)	429.2 (3)	2438.0 (13)	1335.8 (13)
d_{calc}, g/cm^3	1.312	1.256	1.668	1.694
Z	4	1	4	2
λ	Cu K_α	Cu K_α	Mo K_α	Mo K_α
$F(000)$	640	176	1260	704
μ, cm^{-1}	55.24	48.71	13.95	14.72
R_{merg}	5.89	8.28	2.43	2.67
temp, K	108	94	298	93
scan rate, deg/min	2–20	4–20	3–20	3–24
scan technique	Wyckoff	Wyckoff	Wyckoff	Wyckoff
scan range, deg	0.6	0.9	0.9	1.0
cryst size	0.3 × 0.2 × 0.1	0.3 × 0.2 × 0.2	0.2 × 0.1 × 0.1	0.3 × 0.2 × 0.2
reflecns collected	2197	1539	3965	2025
reflecns observed	1584	757	1656	1349
2θ range, deg	3.0–220	3.0–220	3.0–45	3.0–45
R/R_w (obsd data)	4.84/10.30	7.11/11.43	5.39/5.88	5.26/7.74
R/R_w (all data)	5.93/11.57	7.35/12.03	11.35/7.11	6.99/8.58
S	1.33	1.00	1.57	1.44
$\Delta\rho_{max/min}$, e/Å^3	0.36/−0.31	0.54/−0.66	0.73/−0.51	1.19/−0.96
data parm ratio	10.8:1	9.0:1	6.8:1	9.6:1

Table II. Bond Lengths for 1–3[a]

	1	2	3
S(1)–C(2)	1.817 (3)	1.823 (6)	1.803 (7)
C(2)–C(3)	1.504 (4)	1.512 (8)	1.531 (8)
C(3)–S(4)	1.803 (3)	1.835 (6)	1.824 (5)
S(4)–C(5)	1.802 (3)	1.826 (6)	1.818 (5)
C(5)–C(6)	1.505 (3)	1.536 (8)	1.541 (7)
C(6)–C(7)	1.518 (3)	1.542 (8)	1.537 (9)
C(7)–S(8)	1.812 (3)	1.803 (7)	1.820 (5)
S(8)–C(9)		1.810 (6)	
C(9)–C(10)		1.500 (8)	
C(10)–S(11)		1.803 (7)	
S(11)–C(12)		1.822 (6)	
C(12)–C(13)		1.516 (8)	
C(13)–C(14)		1.510 (8)	
C(14)–S(1)		1.832 (6)	

[a] The data for compound **1** (α form) are taken from ref 13a. Because of crystallographic symmetry, the omitted values in the lower half of the table for **1** and **3** occur in the same sequence as those printed in the upper half. The backbone atoms in all macrocycles are numbered according to IUPAC convention; thus, in **2** carbon 6 bears the *gem*-dimethyl pair, and in **3** carbons 6 and 13 bear *gem*-dimethyl pairs.

of polythioether skeletal modifications on the chelation of thiophilic metal ions. Interest in the sulfur-based chelators may have been dampened by early reports indicating that macrocyclic enhancements in this family of ligands are relatively modest[5,6] or even nonexistent.[7] Among oxygen-based ligands, large improvements in cation-binding strength have been achieved simply by converting a linear array of ligating atoms into a macrocyclic array.[8]

Table III. Bond Angles for 1–3[a]

	1	2	3
S(1)–C(2)–C(3)	113.4 (2)	116.5 (4)	110.6 (4)
C(2)–C(3)–S(4)	114.1 (2)	111.1 (4)	114.7 (4)
C(3)–S(4)–C(5)	103.6 (1)	96.8 (3)	98.3 (3)
S(4)–C(5)–C(6)	115.1 (2)	114.0 (4)	114.1 (4)
C(5)–C(6)–C(7)	111.6 (2)	111.3 (5)	110.5 (4)
C(6)–C(7)–S(8)	114.1 (2)	116.9 (4)	114.3 (4)
C(7)–S(8)–C(9)	102.2 (1)	102.6 (3)	97.9 (3)
S(8)–C(9)–C(10)		113.6 (4)	
C(9)–C(10)–S(11)		116.1 (4)	
C(10)–S(11)–C(12)		102.5 (3)	
S(11)–C(12)–C(13)		115.6 (4)	
C(12)–C(13)–C(14)		111.8 (5)	
C(13)–C(14)–S(1)		115.4 (4)	
C(14)–S(1)–C(2)		103.4 (3)	

[a] The data for compound **1** (α form) are taken from ref 13a. Because of crystallographic symmetry, the omitted values in the lower half of the table for **1** and **3** occur in the same sequence as those printed in the upper half. The backbone atoms in all macrocycles are numbered according to IUPAC convention; thus, in **2** carbon 6 bears the *gem*-dimethyl pair, and in **3** carbons 6 and 13 bear *gem*-dimethyl pairs.

Table IV. Bond Lengths for **1**-Ni(II), **2**-Ni(II) and **3**-Ni(II)[a]

	1 + Ni	2 + Ni	3 + Ni
Ni–S(1)	2.178 (1)	2.172 (4)	2.176 (2)
Ni–S(4)	2.175 (1)	2.179 (4)	2.184 (2)
Ni–S(8)		2.182 (4)	
Ni–S(11)		2.179 (4)	
S(1)–C(2)	1.808 (5)	1.810 (12)	1.826 (8)
C(2)–C(3)	1.489 (8)	1.509 (16)	1.509 (10)
C(3)–S(4)	1.821 (6)	1.816 (14)	1.811 (8)
S(4)–C(5)	1.804 (6)	1.807 (10)	1.822 (7)
C(5)–C(6)	1.520 (8)	1.516 (18)	1.558 (10)
C(6)–C(7)	1.519 (8)	1.538 (16)	1.526 (10)
C(7)–S(8)	1.800 (5)	1.810 (11)	1.824 (7)
S(8)–C(9)		1.818 (12)	
C(9)–C(10)		1.512 (16)	
C(10)–S(11)		1.800 (14)	
S(11)–C(12)		1.814 (12)	
C(12)–C(13)		1.506 (22)	
C(13)–C(14)		1.528 (19)	
C(14)–S(1)		1.824 (13)	

[a] The data for **1**-Ni(II) are taken from ref 16. Because of crystallographic symmetry, the omitted values in the lower half of the table for **1**-Ni(II) and **3**-Ni(II) occur in the same sequence as those printed in the upper half. The backbone atoms in all macrocycles are numbered according to IUPAC convention; thus, in **2** carbon 6 bears the *gem*-dimethyl pair, and in **3** carbons 6 and 13 bear *gem*-dimethyl pairs.

Differences between the chelating behavior of polyethers and structurally analogous polythioethers have many possible origins, including differences in the coordination requirements of the target ions and in the solvation properties of the ligands themselves.[9] One particularly intriguing source of variation between these two classes of complexing agents lies in the inherent conformational preferences of the constituent bonds. Chelating polyethers often contain repeating ethylene oxide units, the CO–CC bonds of which intrinsically prefer anti dispositions,[10] while the OC–CO bonds favor gauche dispositions.[11] The inherent preferences of the analogous thioether torsional units are just the opposite: CS–CC prefers gauche and SC–CS favors anti.[2,12] The aggregate effect of such preferences in macrocyclic ethylene oxide oligomers (e.g., the crown ethers) favors conformations in which most or all of the oxygen atoms have a lone pair pointed toward the center of the

(4) (a) Cram, D. J. *Angew. Chem., Int. Ed. Engl.* **1988**, *27*, 1009, and references therein. (b) Lehn, J.-M. *Science* **1985**, *227*, 849, and references therein.

(5) Smith, G. F.; Margerum, D. W. *J. Chem. Soc., Chem. Commun.* **1975**, 807.

(6) Sokol, L. S. W. L.; Ochrymowycz, L. A.; Rorabacher, D. B. *Inorg. Chem.* **1981**, *20*, 3189.

(7) Jones, T. E.; Sokol, L. S. W. L.; Rorabacher, D. B.; Glick, M. D. *J. Chem. Soc., Chem. Commun.* **1979**, 140.

(8) (a) Lamb, J. D.; Izatt, R. M.; Christensen, J. J.; Eatough, D. J. In *Coordination Chemistry of Macrocyclic Compounds*; Melson, G. A., Ed., Plenum Press: New York, 1979; Chapter 3. (b) Izatt, R. M.; Bradshaw, J. S.; Nielsen, S. A.; Lamb, J. D.; Christensen, J. J.; Sen, D. *Chem. Rev.* **1985**, *85*, 271.

(9) Hinz, F. P.; Margerum, D. W. *J. Am. Chem. Soc.* **1974**, *96*, 4993.

(10) (a) Vögtle, F.; Weber, E. *Angew. Chem., Int. Ed. Engl.* **1979**, *18*, 753, and references therein; (b) Dale, J. *Isr. J. Chem.* **1980**, *20*, 1, and references therein.

(11) (a) Wolfe, S. *Acc. Chem. Res.* **1972**, *5*, 102. (b) Juaristi, E. *J. Chem. Ed.* **1979**, *56*, 438.

(12) Desper, J. M.; Powell, D. R.; Gellman, S. H. *J. Am. Chem. Soc.* **1990**, *112*, 1234 and references therein.

Table V. Bond Angles for **1**-Ni(II), **2**-Ni(II) and **3**-Ni(II)[a]

	1 + Ni	2 + Ni	3 + Ni
S(1)-Ni-S(4)	89.8 (1)	90.8 (1)	91.0 (1)
S(1)-Ni-S(8)	180	180.0 (5)	180
S(1)-Ni-S(11)	90.2 (1)	89.4 (1)	89.0 (1)
S(4)-Ni-S(8)	90.2 (1)	89.1 (1)	89.0 (1)
S(4)-Ni-S(11)	180	178.9 (1)	180
S(8)-Ni-S(11)	89.8 (1)	90.7 (1)	91.0 (1)
S(1)-C(2)-C(3)	106.8 (2)	107.7 (7)	106.8 (5)
C(2)-C(3)-S(4)	106.2 (2)	107.2 (10)	107.3 (5)
C(3)-S(4)-C(5)	102.8 (3)	102.8 (6)	101.8 (3)
S(4)-C(5)-C(6)	110.6 (4)	113.8 (9)	112.9 (5)
C(5)-C(6)-C(7)	115.0 (4)	112.3 (9)	111.2 (6)
C(6)-C(7)-S(8)	111.5 (3)	114.5 (7)	113.8 (5)
C(7)-S(8)-C(9)	102.6 (2)	100.9 (5)	101.7 (3)
S(8)-C(9)-C(10)		107.3 (7)	
C(9)-C(10)-S(11)		107.6 (10)	
C(10)-S(11)-C(12)		103.4 (7)	
S(11)-C(12)-C(13)		111.9 (10)	
C(12)-C(13)-C(14)		114.6 (11)	
C(13)-C(14)-S(1)		110.7 (8)	
C(14)-S(1)-C(2)		102.0 (5)	

[a] The data for **1**-Ni(II) are taken from ref 16. Because of crystallographic symmetry, the omitted values in the lower half of the table for **1**-Ni(II) and **3**-Ni(II) occur in the same sequence as those printed in the upper half. The backbone atoms in all macrocycles are numbered according to IUPAC convention; thus, in **2** carbon 6 bears the *gem*-dimethyl pair, and in **3** carbons 6 and 13 bear *gem*-dimethyl pairs.

ring.[10b] In macrocyclic ethylene sulfide oligomers, however, the sulfur atoms tend to adopt "exodentate" positions, in which both lone pairs are pointed away from the center of the ring.[13] (This exodentate tendency remains when additional methylenes are inserted between sulfur atoms, because the CC–CS and CC–CC torsional units prefer anti conformations.)

Because of the intrinsic torsional preferences of CS–CC, SC–CS, and SC–CC units, simple polymethylene spacing elements are not optimal building blocks for thioether-based complexing agents.[12] We have begun to explore alternative linking segments that promote ligand backbone conformations in which the sulfur atoms adopt endodentate positions,[1,14] and we now describe the salutary effects of incorporating 2-*gem*-dimethyl-substituted propylene spacers into a 14-membered macrocyclic tetrathioether skeleton.[15] We find that Ni(II) affinity steadily increases across the series **1**–**3**, in nitromethane solution. Comparison of crystallographic data we have obtained for **2** and **3** and their Ni(II) complexes with previously reported structures of **1**[13a] and its Ni(II) complex[16] suggests that the *gem*-dimethyl substituents have a profound effect on the conformational preference of the macrocyclic backbone, favoring conformations in which the sulfur atoms are preorganized for metal ion chelation.

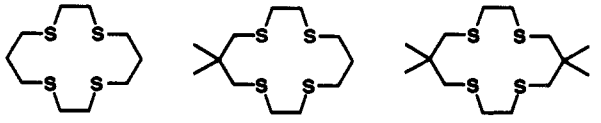

1 **2** **3**

Results and Discussion

Synthesis. Our preparative routes to **2** and **3** are summarized in Scheme I. Starting materials **4**, **5**, and **6** have been previously reported; appropriate references and synthetic details may be found in the Experimental Section. We can find no mention of **2** in the literature prior to our own work. Complexes of **3** with Rh(I)[17] and Ru(II)[18] have been reported, but we have been unable to locate any reference to the preparation or characterization of the ligand itself. The $Ni(ClO_4)_2$ complexes of **2** and **3** were prepared by standard methods.[19]

Table VI. Crystallographically Observed Torsion Angles for Tetrathioethers **1**, **2**, and **3** and for Their Ni(II) Complexes[a]

	1	+Ni	2	+Ni	3	+Ni
S(1)-C(2)-C(3)-S(4)	-176	-61	58	-58	71	-60
C(2)-C(3)-S(4)-C(5)	-60	159	162	155	75	156
C(3)-S(4)-C(5)-C(6)	-62	-175	165	-178	-161	-178
S(4)-C(5)-C(6)-C(7)	178	71	-65	67	59	69
C(5)-C(6)-C(7)-S(8)	177	-72	-60	-68	59	-69
C(6)-C(7)-S(8)-C(9)	63	178	104	176	-156	177
C(7)-S(8)-C(9)-C(10)	67	-157	72	-155	-167	-156
S(8)-C(9)-C(10)-S(11)			173	59		
C(9)-C(10)-S(11)-C(12)			64	-156		
C(10)-S(11)-C(12)-C(13)			-99	177		
S(11)-C(12)-C(13)-C(14)			-168	-70		
C(12)-C(13)-C(14)-S(1)			-54	71		
C(13)-C(14)-S(1)-C(2)			-84	-177		
C(14)-S(1)-C(2)-C(3)			76	156		

[a] The data for **1** (α form) are taken from ref 13a, and the data for **1**-Ni(II) are taken from ref 16. Because of crystallographic symmetry, the omitted torsion angles in the lower half of the table for **1**, **1**-Ni(II), **3**, and **3**-Ni(II) occur in the same sequence as those printed in the upper half, but with change of sign. The backbone atoms in all macrocycles are numbered according to IUPAC convention; thus, in **2** carbon 6 bears the *gem*-dimethyl pair, and in **3** carbons 6 and 13 bear *gem*-dimethyl pairs.

Scheme I

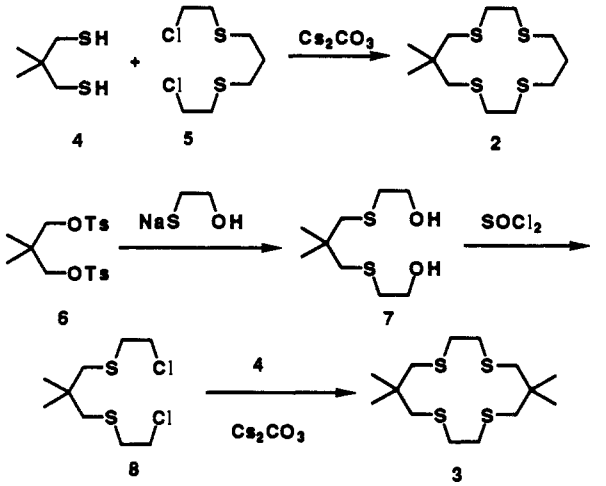

Crystal Structures. Data collection and refinement for the four new structures are summarized in Table I. Bond lengths and angles for the metal-free macrocycles are given in Tables II and III, respectively, and analogous data for the Ni(II) complexes are given in Tables IV and V. Macrocyclic torsion angles are given in Table VI. In Tables II–VI, data for **1**[13a,16] are included for comparison. A single CH_3NO_2 molecule is incorporated in the asymmetric unit of crystalline **2**-$Ni(ClO_4)_2$. Two molecules of $ClCH_2CH_2Cl$ are contained in the unit cell of **3**-$Ni(ClO_4)_2$ (one per nickel–thioether complex).

The carbon–carbon and carbon–sulfur bond lengths in crystalline **2** and **3** fall in the expected ranges, based on many previously reported thioether structures (Table II). The C–C–C, C–S–C, and S–C–C angles in these structures are also typical (Table III). The term "Thorpe–Ingold effect" has been used to describe bond angle compression observed upon *gem*-dialkyl

(13) (a) DeSimone, R. E.; Glick, M. D. *J. Am. Chem. Soc.* **1975**, *98*, 762. (b) Wolf, R. E.; Hartman, J. R.; Storey, J. M. E.; Foxman, B. M.; Cooper, S. R. *J. Am. Chem. Soc.* **1987**, *109*, 4328.

(14) Desper, J. M.; Gellman, S. H. *J. Am. Chem. Soc.* **1991**, *113*, 704.

(15) 2,2-*gem*-Dialkyl-1,3-propanediamines form more stable complexes with Ni(II) than does 1,3-propanediamine itself, see: (a) Hares, G. B.; Fernelius, W. C.; Douglas, B. E. *J. Am. Chem. Soc.* **1956**, *78*, 1816. (b) Newman, M. S.; Busch, D. H.; Cheney, G. E.; Gustafson, C. R. *Inorg. Chem.* **1972**, *11*, 2890.

(16) Davis, P. H.; White, L. K.; Belford, R. L. *Inorg. Chem.* **1975**, *14*, 1753.

(17) Yoshida, Y.; Ueda, T.; Adachi, T.; Yamamoto, K.; Higuchi, T. *J. Chem. Soc., Chem. Commun.* **1985**, 1137.

(18) Ueda, T.; Tamanaka, H.; Adachi, T.; Yoshida, T. *Chem. Lett.* **1988**, 525.

(19) Rosen, W.; Busch, D. H. *Inorg. Chem.* **1970**, *9*, 262.

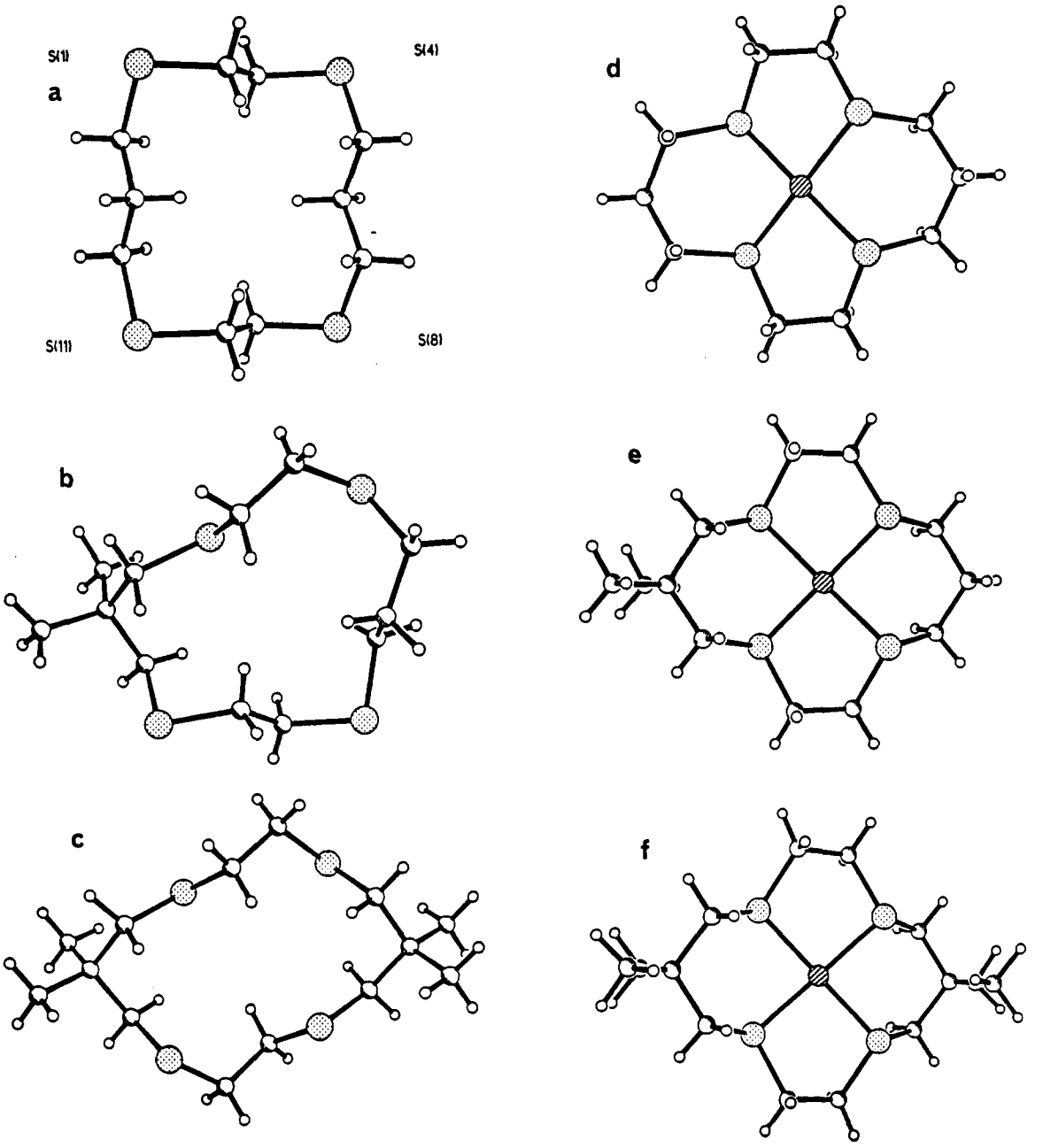

Figure 1. Ball-and-stick representation of the crystallographically observed thioether conformations: (a) macrocycle **1** (α form, ref 13a), (b) macrocycle **2**, (c) macrocycle **3**, (d) **1**-Ni(II) (BF_4 counterions not shown, ref 16), (e) **2**-Ni (ClO_4 counterions not shown), (f) **3**-Ni (ClO_4 counterions not shown).

substitution of an sp^3 carbon.[20] Angle compression associated with the *gem*-dimethyl substitution in **2** and **3** is relatively modest. In **2**, the *gem*-dimethyl-substituted angle C_5–C_6–C_7 = 111.3 ± 0.5°, while the unsubstituted angle C_{12}–C_{13}–C_{14} = 111.8 ± 0.5°. In **3**, the *gem*-dimethyl-substituted angle C_5–C_6–C_7 = 110.5 ± 0.4°. The C_5–C_6–C_7 angles in the three crystal forms of **1** reported previously fall between 111.6 ± 0.2 and 112.1 ± 0.6°.[13a]

Inspection of the metal-free structures of **1**, **2**, and **3** (Figure 1a–c) reveals three very different 14-membered ring backbone conformations. The α and β_1 crystalline forms of **1** observed by DeSimone and Glick have both SC–CS bonds and all four SC–CC bonds anti, and all eight CS–CC bonds are gauche.[13a] In **2**, one of the SC–CS and three of the SC–CC bonds are gauche, and two of the CS–CC bonds are anti. In **3**, both SC–CS and all four SC–CC bonds are gauche, and six of the eight CS–CC bonds are anti (Table VI).

The solid-state data for **1**–**3** (Figure 1a–c) indicate that placement of a *gem*-dimethyl pair at the center methylene of a propylene moiety induces the two nearest sulfur atoms to direct one lone pair each toward the macrocycle's central cavity. Consistent patterns in the sequences of skeletal torsion angles (Table VI) along analogous segments of **1**–**3** suggest that lattice packing effects are not the principal origin of these conformational trends, but rather that the crystallographically detected macrocycle folding patterns are largely a result of the interplay between the intrinsic torsional potentials of the individual bonds and the constraints imposed by the 14-membered ring. Roughly half of the macrocyclic backbone of **2** (S_1 to S_8), containing the *gem*-dimethyl pair, displays a sequence of five torsion angles that is very similar to the corresponding sequence observed in an analogous stretch of bonds in the backbone of **3** (S_4 "backwards" to S_{11}). Much of the remaining backbone of **2** (S_8 to C_{14}) displays torsion angles that are typical for unsubstituted SC–CS, SC–CC, and CS–CC bonds, as observed in **1**.[13a]

The *gem*-dimethyl-induced backbone rearrangements of the 14-membered ring can be rationalized to some extent by considering the effect of the bulky methyl groups on the local torsional potentials. The CS–CC(Me_2) torsional units are expected to prefer anti dispositions (to avoid 1,5 carbon–carbon repulsions), in contrast to the gauche preference of the analogous CS–CC(H_2)

units. The SC–CC torsion angles should also be affected by the bulky substituents. The SC–C(H_2)C torsional unit has a significant intrinsic preference for anti over gauche dispositions, but there should be little or no energetic difference between anti and gauche dispositions of SC–C(Me_2)C (where gauche and anti are defined with respect to the macrocyclic atoms), because in the latter case a 1,4 sulfur–carbon interaction is unavoidable. (This analysis of the conformation-directing effects of the *gem*-dimethyl substituents in crystalline **1–3** is related to the enthalpy-based arguments used by Allinger and Zalkow to explain the effects of alkyl substitution on the relative stabilities of analogous linear and six-membered ring hydrocarbons.[21])

The constraints imposed by the macrocyclic connectivity must also be taken into account for a complete rationalization of the *gem*-dimethyl-induced changes in **2** and **3** relative to **1**. The intrinsic anti preference of the SC–CS unit is manifested in the structure of **1**, but one of the two SC–CS units in **2** and both in **3** are gauche. The occurrence of gauche SC–CS units in crystalline **2** and **3** presumably reflects unavoidable strain in these macrocycles, resulting indirectly from the presence of the sterically demanding *gem*-dimethyl pairs.

In contrast to the conformational variation observed among the metal-free tetrathioethers, the Ni(II) complexes of **1–3** display remarkably similar 14-membered ring conformations (Figure 1d–f). As indicated by the data given in Table VI, analogous macrocycle torsion angles vary by only a few degrees from one chelate structure to the next. The bond lengths in **2**-Ni(ClO_4)$_2$ and **3**-Ni(ClO_4)$_2$ (Table IV) are similar to the analogous lengths reported for **1**-Ni(BF_4)$_2$.[16] It is noteworthy that the Ni–S bond lengths in the two new structures (2.17–2.18 Å) do not vary significantly from the Ni–S lengths in the Ni(II) complex of **1**.

From a consideration of the gauche vs anti energetics of CS–CC, SC–CC, and SC–CS bonds in simple thioethers (eqs 1–3 below), one predicts that, in the absence of the chelated metal ion, the macrocycle conformation observed for **1**-Ni(II) would be significantly destabilized enthalpically relative to the conformation observed crystallographically for metal-free **1**.

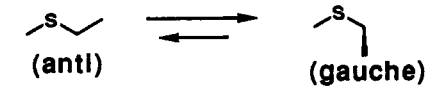

(1)

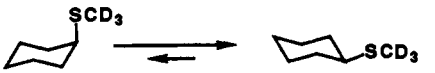

(2)

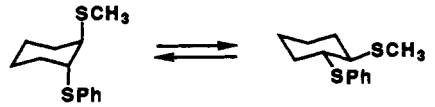

(3)

The conformational preference of the CS–CC unit is manifested in the behavior of $CH_3SCH_2CH_3$ (eq 1). Several research groups have studied this molecule in the gas phase, and all find a small enthalpic advantage for gauche over anti (0.05–0.2 kcal/mol).[22] The conformational preference of the SC–CC unit determines the preferred form of (methylthio)cyclohexane (eq 2). Equatorial and axial dispositions of the SCD_3 group on a cyclohexane ring are reported to differ in $\Delta G°$ at −79 °C by 1.1 kcal/mol (equatorial favored).[23] If we assume that the entropies of the alternative chair conformations of this molecule are similar,[24] this result implies an enthalpic preference of 0.5–0.6 kcal/mol for anti over gauche SC–CC, because axial positioning requires two gauche SC–CC interactions that are not present in the equatorial conformer. The conformational preference of the SC–CS unit has been studied indirectly by Zefirov et al., who reported that $\Delta G°$ for the conformational equilibrium shown in eq 3 varies between 0.1 and −0.4 kcal/mol at room temperature, depending upon solvent.[25] If we assume that the *A* value for SCH_3 and SPh are similar and that the entropies of the alternative chair conformations are similar,[24] then this observation of Zefirov and coworkers suggests that the gauche form of SC–CS is enthalpically destabilized by roughly 2.0 kcal/mol relative to the anti form.

In aggregate, the results for the systems in eq 1–3 imply that the macrocycle conformation observed for **1**-Ni(II) may experience several kcal/mol of torsional strain, relative to the conformation of metal-free **1**. Figure 1 shows that the conformational rearrangement necessary to convert the crystallographically observed metal-free macrocycle conformation into the Ni(II)-bound conformation diminishes progressively in scope across the series **1–3**. The structural data therefore suggest that the torsional enthalpy cost associated with Ni(II) complex formation decreases with the introduction of each *gem*-dimethyl pair.

Angle strain factors may oppose the chelation-enhancing effects of the *gem*-dimethyl-induced torsional preorganization across the series **1–3**. Within the six-membered chelate rings of the Ni(II) complexes, there is a consistent difference between the sequence of bond angles along S–C–C(H_2)–C–S segments and the sequence along S–C–C(Me_2)–C–S segments (Table V). The published data for **1**-Ni(BF_4)$_2$ show 110.6 ± 0.4, 115.0 ± 0.4, and 111.5 ± 0.3° for sequential S–C–C(H_2), C–C(H_2)–C, and C(H_2)–C–S angles.[16] For **3**-Ni(ClO_4)$_2$, we observe 112.9 ± 0.5, 111.2 ± 0.6, and 113.8 ± 0.5° for the corresponding S–C–C(Me_2), C–C(Me_2)–C, and C(Me_2)–C–S angles. These alternative patterns in six-membered chelate rings, C–C–S larger than C–C–C when a *gem*-dimethyl pair is present but C–C–S smaller than C–C–C in the absence of a *gem*-dimethyl pair, seem to be directly related to the presence or absence of the *gem*-dimethyl pair, because each characteristic pattern is observed in the appropriate portion of **2**-Ni(ClO_4)$_2$. In all cases, the S–C–C/C–C–C/C–C–S bond angle pattern observed in the unsubstituted propylene segments varies much more between metal-free and metal-bound forms than does the bond angle pattern observed in the *gem*-dimethyl-substituted propylene segments. Thus, the central C–C–C angle of the unsubstituted segments widens significantly upon Ni(II) complexation, but the analogous angle of the *gem*-dimethyl-substituted segments widens only slightly. Further, the S–C–C angles of the unsubstituted segments narrow substantially when the ion is bound, but the analogous angles of the *gem*-dimethyl-substituted segments tend to narrow to a lesser extent. These bond angle changes in the unsubstituted propylene segments presumably represent an energetically favorable response to the structural demands imposed by metal ion chelation; therefore, the lack of bond angle change in the *gem*-dimethyl-substituted segments suggests the existence of bond angle strain in **2**-Ni(II) and **3**-Ni(II), relative to **1**-Ni(II).

Solution Structures. ^{1}H NMR data imply that **1–3** all experience rapid conformational averaging in CD_3NO_2 (room temperature). In contrast, conformational interconversions of the Ni(ClO_4)$_2$ complexes of **1–3** are slow on the NMR time scale under these conditions. On the basis of ^{13}C NMR data, Moore et al. proposed the existence of two slowly interchanging metal-bound macrocycle conformations for **1**-Ni(BF_4)$_2$ in CD_3NO_2.[26] Our ^{1}H NMR data are consistent with the existence of two metal-bound conformations for all three Ni(ClO_4)$_2$ complexes.

(20) (a) Beesley, R. M.; Ingold, C. K.; Thorpe, J. F. *J. Chem. Soc.* **1915**, *107*, 1080. (b) For a critical evaluation of the Thorpe–Ingold effect and other effects on reactivity arising from *gem*-dialkyl substitution, see: Kirby, A. J. *Adv. Phys. Org. Chem.* **1980**, *17*, 183. (c) For a very recent discussion of these issues, see: Jung, M. E.; Gervay, J. *J. Am. Chem. Soc.* **1991**, *113*, 224.

(21) Allinger, N. L.; Zalkow, V. *J. Org. Chem.* **1960**, *25*, 701.

(22) (a) Durig, J. R.; Compton, D. A. C.; Jalilian, M. R. *J. Phys. Chem.* **1979**, *83*, 511. (b) Oyanagi, K.; Kuchitsu, K. *Bull. Chem. Soc. Jpn.* **1978**, *51*, 2243. (c) Sakakibara, M.; Matsuura, H.; Harada, I.; Shimanoguchi, T. *Bull. Chem. Soc. Jpn.* **1977**, *50*, 111. (d) Nogami, H.; Sugeta, H.; Miyazawa, T. *Bull. Chem. Soc. Jpn.* **1975**, *48*, 3573. See, also: (e) Fausto, R.; Teixeira-Dias, J. J. C.; Carey, P. R. *J. Mol. Struct.* **1987**, *159*, 137.

(23) Jensen, F. R.; Bushweller, C. H.; Beck, B. H. *J. Am. Chem. Soc.* **1969**, *91*, 344.

(24) The entropy difference between axial and equatorial conformers of isopropylcyclohexane appears to be small but significant, see: Squillacote, M. E. *J. Chem. Soc., Chem. Commun.* **1986**, 1406.

(25) Zefirov, N. S.; Gurvich, L. G.; Shashkov, A. S.; Krimer, M. Z.; Vorob'eva, E. A. *Tetrahedron* **1976**, *32*, 1211.

(26) (a) Herron, N.; Horwarth, O. W.; Moore, P. *Inorg. Chim. Acta* **1976**, *20*, L43. (b) Two RH(l)-complexed conformations of **3** have been detected by ^{1}H NMR in DMSO; see ref 17.

Table VII. (Gauche–Anti) Conformational Energy Differences, in kcal/mol, Calculated for Three Thioether Torsional Units with Three Common Molecular Mechanics Force Fields

torsion	MM2[a]	AMBER[a]	OPLS/A[a]	exptl
CS–CC[b]	+0.37	+0.26	+0.47	−0.05–0.2[e]
SC–CC[c]	+0.55	+0.62	−0.11	+0.54[f]
SC–CS[d]	+1.2	−1.7	+1.4	+2.2[g]

[a] As implemented MACROMODEL V2.5 (ref 35). [b] As manifested in $CH_3SCH_2CH_3$ (eq 1 in text). [c] As manifested in (methylthio)cyclohexane (eq 2 in text). [d] As manifested in the central bond of $CH_3SCH_2CH_2SCH_3$; the CS–CC bonds were held in the anti conformations during these calculations. [e] Range of enthalpies reported for (gauche–anti) $CH_3SCH_2CH_3$ in the gas phase (ref 22). [f] On the basis of the reported Gibbs free energy difference between axial and equatorial CD_3S on the cyclohexane ring (ref 23). [g] On the basis of the reported Gibbs free energy difference between the diaxial and diequatorial forms of the dithioether shown in eq 3 in the text (ref 25).

We observe selective broadening of one set of ^1H NMR signals for the CH_2 groups adjacent to sulfur atoms (the other set of these methylene resonances is sharp); an analogous selective broadening of ^{13}C signals was reported by Moore and co-workers.[27] This broadening makes detailed analysis of the methylene region difficult. For **2** and **3**, the clearest spectroscopic indications of slow conformational exchange are the methyl signals: each ligand shows only one methyl proton singlet in the absence of Ni(II) (1.00–1.01 ppm), but each shows four methyl proton singlets (1.19–1.43 ppm) when Ni(II) is present.

Moore et al. hypothesized that one of the two conformations of **1**-Ni(II) present in CD_3NO_2 is that which had previously been observed crystallographically for **1**-Ni(II) (Figure 1a).[26a] This macrocycle conformation has subsequently been designated anti,[2b] because the two six-membered chelate rings extend out on opposite sides of the plane defined by the four sulfur atoms and the bound metal. The other conformation detected in solution was proposed to have both six-membered rings on the same side of the coordination plane,[26a] a conformation that has been designated syn.[2b] Conformations of this second type have recently been observed crystallographically for **1**-Rh(I),[17] **3**-Ru(II),[18] **2**-Cu(II),[14] and **3**-Cu(II).[14]

When any of macrocycles **1–3** is mixed with 1 equiv of $Ni(ClO_4)_2$ in CD_3NO_2, we can detect no signals for metal-free ligand by ^1H NMR.[28] When 1 equiv of $Ni(ClO_4)_2$ (12.5 mM) is mixed with 2 equiv of any of the macrocycles **1–3**, distinct signals for both metal-free and coordinated ligand are observed in 1:1 ratio. This observation indicates that exchange of Ni(II) ions between individual tetrathioether molecules is slow on the NMR time scale, and that 2:1 (ligand/metal) complexes do not form to any significant extent under these conditions.

Relative Ni(II) Affinities in Solution. The ratio of the Ni(II) binding constants of the parent macrocycle **1** and either of the methylated compounds, **2** or **3**, was determined by ^1H NMR in CD_3NO_2 from competition experiments. The success of this approach depends upon three features of the experimental system: (1) exchange between metal-free and metal-bound forms of **1–3** is slow; (2) binding of Ni(II) by 1 equiv of any of the three macrocycles is essentially complete in CD_3NO_2 in the concentration ranges employed; (3) the methyl resonances of the metal-free and chelated forms of **2** or **3** are sufficiently well isolated from one another, and from all other signals, to allow accurate integration. Competition experiments were performed by dissolving 1 equiv of $Ni(ClO_4)_2$, 1 equiv of **1**, and 1 equiv of **2** or **3** in sufficient CD_3NO_2 for a final solution containing each component at 12.5 mM. These solutions required several days at room temperature to reach equilibrium, at which point the ratio of metal-bound to metal-free *methylated* ligand (**2** or **3**) was determined from the ratio of the integration of the singlet at 1.00–1.01 ppm to the integration of the four singlets in the range 1.19–1.43 ppm (Figure 2).[29]

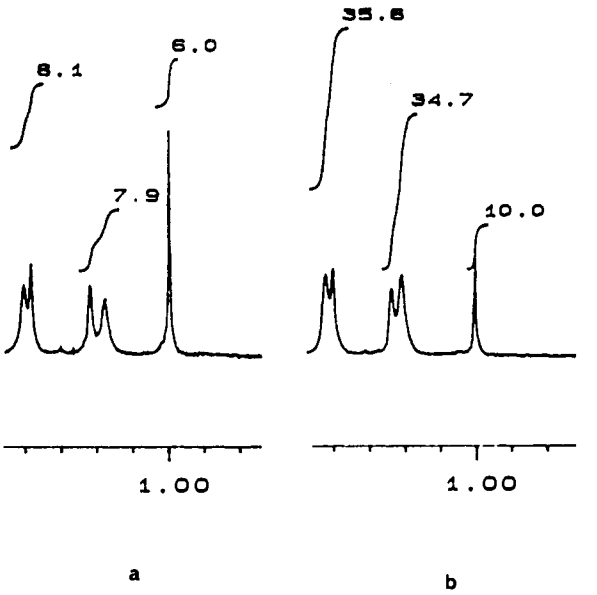

Figure 2. CH_3 (0.8–1.4 ppm) region of the ^1H NMR spectrum of Ni(II) binding competition experiment solutions (CD_3NO_2, room temperature). (a) Sample containing 1:1:1 $Ni(ClO_4)_2$/**1**/**2**, each component 12.5 mM; the signal at 1.00 ppm arises from metal-free **2**, and the signals above 1.1 ppm arise from **2**-Ni. (b) Sample containing 1:1:1 $Ni(ClO_4)_2$/**1**/**3**, each component 12.5 mM; the signal at 1.01 ppm arises from metal-free **3**, and the signals above 1.1 ppm arise from **3**-Ni. The spectra were obtained on a Bruker WP-200 spectrometer, FIDs were processed and integrated on an IBM PC, using the PCNMR Plus software package. The numbers shown for individual integrals have no absolute value, but within each spectrum these numbers accurately represent the relative areas of the integrated peaks. Details of sample preparation may be found in the Experimental Section.

For a competition experiment involving **1** and **2**, it can be demonstrated that the integration ratio of the metal-bound and metal-free methyl signals is equal to the square root of the ratio of association constants for Ni(II) complexation by these two ligands. (The analysis of the competition experiment involving **1** and **3** is completely analogous.) The situation in the competition experiment solution can be described by a single equilibrium (eq 4).

$$\textbf{1}\text{-Ni(II)} + \textbf{2} \overset{K_{12}}{\rightleftharpoons} \textbf{1} + \textbf{2}\text{-Ni(II)} \tag{4}$$

The equilibrium constant (K_{12}) for the process indicated in eq 4 is defined in eq 5.

$$K_{12} = \frac{[\textbf{2}\text{-Ni(II)}][\textbf{1}]}{[\textbf{1}\text{-Ni(II)}][\textbf{2}]} \tag{5}$$

K_{12} is equal to the ratio of equilibrium constants for complexation of Ni(II) by **1** and **2** alone, as indicated in eqs 6–8.

$$\textbf{1} + \text{Ni(II)} \overset{K_1}{\rightleftharpoons} \textbf{1}\text{-Ni(II)} \tag{6}$$

$$\textbf{2} + \text{Ni(II)} \overset{K_2}{\rightleftharpoons} \textbf{2}\text{-Ni(II)} \tag{7}$$

$$K_{12} = \frac{K_2}{K_1} \tag{8}$$

(27) Moore et al. (ref 26a) attributed the selective broadening of NMR resonances to "the formation of a paramagnetic five- or six-coordinate complex", involving interaction of water (present in trace amounts) with one of the two chelate geometries in solution.

(28) The fact that we are unable to detect any metal-free macrocycle in a CD_3NO_2 solution containing 10 mM Ni(II) and 10 mM **2** or **3** indicates that the absolute binding constants of these ligands in this solvent are $>10^5$ M^{-1}, since the methyl singlet of the metal-free forms would be detectable at concentrations as low as 0.1–0.5 mM.

(29) In order to verify that the solutions used to measure Ni(II) association constant ratios had indeed reached equilibrium, parallel samples were prepared by starting either with 1 equiv of **1** plus 1 equiv of **2**-$Ni^{II}(ClO_4)_2$, or with 1 equiv of **2** plus 1 equiv of **1**-$Ni^{II}(ClO_4)_2$. Immediately after preparation, these solutions showed very different ratios of metal-free to metal-bound **2** by ^1H NMR. After several days, however, the two solutions converged to a common ratio of 2.7. Similar controls gave analogous results for **1** vs **3**.

The absence of any unbound Ni(II) ions and the equal concentrations of Ni(II) ions, **1** and **2**, require that [**2**-Ni(II)] = [**1**] and [**1**-Ni(II)] = [**2**]. Applying these constraints to eq 5, we find

$$K_{12} = \frac{[\mathbf{2}\text{-Ni(II)}]^2}{[\mathbf{2}]^2} \tag{9}$$

The methyl signal integration ratio measured in the ^{1}H NMR competition experiments is [**2**-Ni(II)]/[**2**]; eq 9 tells us that this experimentally determined value is the square root of the ratio of the Ni(II) binding constants of **2** and **1**.

^{1}H NMR data from a representative competition experiment involving **1** and **2** are shown in Figure 2a; analogous data from an experiment involving **1** and **3** are shown in Figure 2b. The integration ratio of metal-bound to metal-free methyl signals in Figure 2a is 2.7, indicating that K_{12} = 7.3. The integration ratio in Figure 2b is 7.0, indicating that K_{13} = 49.[30]

Smith and Margerum employed a different method to study the relative Ni(II) affinities of **1** and an analogous acyclic tetrathioether, **9**, in nitromethane.[5] Their approach involved the use of excess quantities of diol **10** to prevent complete Ni(II) complexation by **1** or **9**. In separate experiments, Smith and Margerum deduced the ratio of the Ni(II) binding constant of **1** or **9** to the Ni(II) binding constant of **10** by monitoring a UV absorption unique to the square-planar tetrathioether-Ni(II) complexes, as a function of the amount of **1**-Ni(II) or **9**-Ni(II) added to a solution containing an excess of **10**. Smith and Margerum reported that **1** binds Ni(II) 180 times more strongly than does **9**.[5] In our hands, the reproducibility of this method is too low to be of use in comparing the Ni(II) affinities of **1**–**3**.[31]

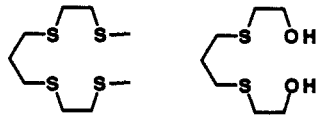

9 **10**

Molecular Mechanics Calculations. In principle, molecular mechanics calculations[32] should allow one to probe the effect of *gem*-dimethyl substituents on the relative enthalpic stabilities of alternative 14-membered ring conformations of **1**–**3**. Before performing such calculations on the macrocyclic tetrathioethers, however, one must evaluate a given force field's ability to reproduce energetic data reported for simpler thioethers containing the key torsional units. We have examined the calculated enthalpic differences between the gauche and anti forms of CS–CC, SC–CC, and SC–CS torsional units using the MM2,[32] AMBER,[33] and OPLS/A[34] force fields as implemented by MACROMODEL V2.5.[35] For CS–CC and SC–CC, we used the experimental systems discussed above, $CH_3SCH_2CH_3$ (eq 1) and (methylthio)cyclohexane (eq 2), respectively. For SC–CS, we used CH_3SCH_2-CH_2SCH_3, with the CS–CC units held in anti conformations. As discussed above, data for a derivative of *trans*-cyclohexane-1,2-dithiol (eq 3) suggest that anti SC–CS should be approximately 2 kcal/mol more favorable enthalpically than gauche SC–CS.

Table VII summarizes the results obtained for the three thioether test cases with the three force fields. (In the following discussion, we assume that molecular mechanics energies correspond most closely to experimental enthalpies, rather than Gibbs free energies.) All of the force fields predict the anti conformation of $CH_3SCH_2CH_3$ to be more enthalpically favorable than the gauche, in contrast to the experimental findings.[22] MM2 and AMBER predict that equatorial placement of the methylthio substituent is favored over axial placement on a cyclohexane ring, and both force fields seem to provide an acceptable assessment of the energetic difference between the two conformers,[23] if we assume that there is little entropic contribution to the experimentally measured $\Delta G°$ difference between equatorial and axial (methylthio)cyclohexane.[24] In contrast, OPLS/A predicts that the axial conformer is slightly more favorable enthalpically than the equatorial, in clear contradiction to the experimental results. MM2 and OPLS/A correctly predict that anti conformations of the SC–CS torsional unit are enthalpically more stable than gauche. The magnitude of the predicted anti preference is somewhat smaller for MM2 than for OPLS/A, and both seem to be smaller than expected, based on experimental results.[25] AMBER predicts that the gauche conformation of SC–CS is substantially more stable enthalpically than the anti conformation, which is clearly at odds with experimental observations.[12,25]

Each of the three force fields, as implemented by MACROMODEL V2.5, appears to have significant flaws in its ability to reproduce thioether conformational preferences. Computational analysis of macrocycles **1**–**3** will require a force field that more accurately reproduces thioether torsional potentials.

Conclusions. We have shown that relatively simple peripheral modifications of macrocyclic polythioethers can lead to substantial improvements in Ni(II) complexation. Across the series **1**–**3**, each additional *gem*-dimethyl pair produces a 7-fold enhancement in association constant at room temperature in nitromethane solution, which represents a $\Delta\Delta G°$ of complexation of approximately −1.1 kcal/mol per *gem*-dimethyl pair. These incremental improvements seem to be related to energetic differences among the metal-free ligands. The occurrence of gauche SC–CS torsion angles in the crystallographically observed conformations of metal-free **2** and **3** suggests that these molecules are enthalpically strained relative to **1**. In contrast, the Ni(II)-bound conformations of **2** and **3** do not appear to be torsionally strained relative to the Ni(II)-bound conformation of **1** (**2** and **3** may, however, experience greater bond angle strain than **1** in the Ni(II)-bound state). It seems likely that the increased Ni(II) affinity of the macrocycles bearing *gem*-dimethyl pairs at the 6- and 13-positions results, at least in part, from the decreasing enthalpic stability of the metal-free thioethers across the series **1**–**3**.[36] These findings are important because they demonstrate that the design of new polythioether chelators requires one to take into account the distinctive conformational properties of thioether-containing torsional units.

Experimental Section

Materials. Sodium hydride (60% dispersion), *p*-toluenesulfonyl chloride, 2,2-dimethyl-1,3-propanediol, 2-mercaptoethanol, and cesium carbonate were purchased from Aldrich Chemical Co. Ni(II) salts were obtained as their hydrates from Morton Thiokol. Nitromethane was obtained from Kodak Chemicals and was purified by the method of Olah et al.[37] Acetic anhydride was obtained from EM Industries. Thionyl chloride was obtained from MCB. 1,4,8,11-Tetrathiacyclotetradecane (**1**) was purchased from Aldrich Chemical Co. and was recrystallized before use (EtOH).

Instrumentation. NMR spectra were obtained on a Bruker WP-200 spectrometer. Mass spectra were obtained on a Kratos MS-25 instrument. Infrared spectra were obtained on a Mattson Polaris instrument (KBr). UV spectra were obtained on a Hewlett-Packard 8452A diode array spectrophotometer.

(30) The competition method could not be used to determine K_{23}, because both ligands bear *gem*-dimethyl groups.

(31) Inspection of G. F. Smith's Ph.D. Dissertation (Purdue University, 1975; available from University Microfilms International, Ann Arbor, MI) suggests that the original workers also had problems with reproducibility.

(32) Burkert, U.; Allinger, N. L. *Molecular Mechanics*; American Chemical Society Monograph No. 177, 1982.

(33) Weiner, S.; Kollman, P. A.; Nguyen, D. T.; Case, D. A. *J. Comput. Chem.* **1986**, *7*, 230.

(34) Jorgensen, W. L.; Tirado-Rives, J. *J. Am. Chem. Soc.* **1988**, *110*, 1657.

(35) Mohamadi, F.; Richards, N. G. J.; Guida, W. C.; Liskamp, R.; Lipton, M.; Caufield, C.; Chang, C.; Chang, G.; Hendrickson, T.; Still, W. C. *J. Comput. Chem.* **1990**, *11*, 440.

(36) It is well-established that structural changes that decrease the conformational flexibility of a backbone containing an array of ligating atoms will diminish the entropic barrier to metal ion chelation, provided that the structural changes do not enthalpically disfavor the chelating conformation, see: Cram, D. J. *Angew. Chem., Int. Ed. Engl.* **1986**, *25*, 1039. At present, we have no direct evidence on the relative flexibilities of **1**, **2**, and **3**, and we cannot comment on the significance of entropic preorganization across this series.

(37) Olah, C. A.; Kuhn, S. J.; Flood, S. H.; Hardie, B. A. *J. Am. Chem. Soc.* **1964**, *86*, 1039.

1,3-Bis((*p*-toluenesulfonyl)oxy)-2,2-dimethylpropane (6).[38] Pyridine (100 mL) was chilled in an ice/salt bath, and then *p*-toluenesulfonyl chloride (25.21 g, 132 mmol) was added. A solution of 6.24 g (60 mmol) of 2,2-dimethyl-1,3-propanediol in 30 mL of pyridine was added slowly to the chilled stirred solution, and the mixture was stored overnight at −20 °C. The mixture was then partitioned between 200 mL of $CHCl_3$ and 200 mL of ice/concentrated HCl. The organic layer was washed with 2 × 200 mL of ice/HCl, 200 mL of H_2O, 200 mL of ice/1 M NaOH, and then 200 mL of H_2O. The organic layer was dried over $MgSO_4$ and evaporated, giving a white solid (21.79 g, 88%), which was not further purified: ^1H NMR ($CDCl_3$) δ 0.88 (s, 6 H, CH_3), 2.46 (s, 6 H, CH_3), 3.71 (s, 4 H, OCH_2), 7.35, 7.74 (AB quar, $J \sim 8.3$ Hz, 8 H, aryl CH); EI-MS calcd for $C_{19}H_{24}S_2O_6$ 412.1014, found 412.1019.

5,5-Dimethyl-3,7-dithio-1,9-nonanediol (7). Ethanol (90 mL) was degassed for 20 min with N_2 in a 200-mL flask. Sodium (713 mg, 31 mmol) was weighed under xylenes and allowed to dissolve in the EtOH while the stream of N_2 was maintained. 2-Mercaptoethanol (2.17 mL, 31 mmol) was added, and ditosylate **6** was added (6.00 g, 14.5 mmol). The flask was fitted with a condenser, and the reaction solution was refluxed 72 h under N_2. The solvent was then removed by distillation under aspiration, and the residue was taken up in 50 mL of H_2O/50 mL of $CHCl_3$. The aqueous layer was extracted with 2 × 40 mL of $CHCl_3$, and the combined organic layers were washed with 50 mL of saturated aqueous $NaHCO_3$, dried over $MgSO_4$, and concentrated. The remaining yellow oil was purified by column chromatography (SiO_2/EtOAc), to give a viscous, colorless oil, 1.862 g (57%): ^1H NMR ($CDCl_3$) δ 1.07 (s, 6 H, CH_3), 2.62 (s, 4 H, SCH_2), 2.75 (t, $J = 5.8$ Hz, 4 H, SCH_2), 3.74 (t, $J = 5.8$ Hz, 4 H, OCH_2), 2.38 (br, −OH); EI-MS calcd for $C_9H_{20}O_2S_2$ 224.0905, found 224.0911.

5,5-Dimethyl-1,9-dichloro-3,7-dithiononane (8) (*Warning! Severe Vesicant!*) was prepared by a procedure related to that reported for the analogue without the *gem*-dimethyl pair (**5**).[39] To a solution of 3 mL of $SOCl_2$ in 15 mL of CH_2Cl_2 was added dropwise a solution of diol **7** (2.3 g, 10.2 mmol) in 10 mL of CH_2Cl_2. Bubbling ceased after 5 min; the mixture was stirred an additional 40 min, and then added dropwise to a vigorously stirred solution of 200 mL of saturated aqueous $NaHCO_3$. The mixture was stirred 10 min, the phases were separated, and the aqueous layer was extracted with 2 × 50 mL of CH_2Cl_2. The combined organic layers were washed with 200 mL of saturated aqueous $NaHCO_3$ and dried over $MgSO_4$, and the solvent was removed with a N_2 stream to give a light gold oil, 2.025 g (78%): ^1H NMR ($CDCl_3$) δ 1.04 (s, 6 H, CH_3), 2.62 (s, 4 H, SCH_2), 2.87 (t, $J = 7.9$ Hz, 4 H, SCH_2), 3.63 (t, $J = 7.9$ Hz, 4 H, $ClCH_2$). Because of its hazardous nature, this compound was not further characterized or purified.

6,6-Dimethyl-1,4,8,11-tetrathiocyclotetradecane (2) was prepared by methodology similar to that used by Buter and Kellogg to prepare **1**.[40] To a three-necked, 500-mL, round-bottomed flask fitted with a condenser and a 50-mL addition funnel, under N_2, was added 2.842 g of Cs_2CO_3 (8.72 mmol) and 300 mL of degassed DMF, and the mixture was heated to 80 °C with stirring. Meanwhile, 1.187 g (8.72 mmol) of 2,2-dimethyl-1,3-propanedithiol (**4**)[38] and 2.034 g (8.72 mmol) of mustard **5**[35] were dissolved in 100 mL of degassed DMF, and half of this solution was placed in the addition funnel and added dropwise to the hot Cs_2CO_3 suspension over 4 h. The remaining reagent solution was added to the funnel and allow to add dropwise overnight. The solvent was then removed under vacuum, and the residue was taken up in 100 mL of H_2O/100 mL of $CHCl_3$. The aqueous layer was extracted with 100 mL of $CHCl_3$, and the combined organic layers were dried over $MgSO_4$ and evaporated to a yellow paste, which was purified by column chromatography (24:1 hexane/EtOAc), to give 1.181 g of white solid (45%): mp = 66 °C; ^1H NMR ($CDCl_3$) δ 1.03 (s, 6 H, CH_3), 1.93 (quint, $J = 7$ Hz, 2 H, CH_2), 2.71 (s, 4 H, SCH_2), 2.71 (t, $J = 7$ Hz, 4 H, SCH_2), 2.84 (m, 8 H, SCH_2); IR (KBr) 2958, 2909, 1467, 1450, 1416, 1379, 1362, 1269, 1260, 1192, 1138, 1001, 929, 867, 820, 746, 722, 690 cm^{-1}; EI-MS calcd for $C_{12}H_{24}S_4$ 296.0761, found 296.0765.

6,6,13,13-Tetramethyl-1,4,8,11-tetrathiocyclotetradecane (3) was prepared by methodology similar to that used by Buter and Kellogg to prepare **1**.[40] In a three-necked, 1000-mL flask fitted with a condenser and a 250-mL addition funnel, under N_2, was placed 3.571 g (10.96 mmol) of Cs_2CO_3 and 400 mL of degassed DMF. A solution of 1.493 g (10.96 mmol) of 2,2-dimethyl-1,3-propanedithiol (**4**)[41] and 2.863 g (10.96 mmol) of mustard **8** in 250 mL of degassed DMF was prepared, and half of this solution was placed in the addition funnel. The reaction vessel was warmed to 80 °C, and the reagent solution was added dropwise over 4 h. Additional Cs_2CO_3 (3.571 g, 10.96 mmol) was then added to the reaction flask, and the remainder of the reagent solution was added dropwise overnight. The solvent was then removed by vacuum distillation, and the yellow residue was taken up in 150 mL of H_2O/150 mL of $CHCl_3$. The phases were separated, and the aqueous layer extracted with 2 × 50 mL of $CHCl_3$. The combined organic layers were dried over $MgSO_4$ and evaporated to a white/yellow paste, which was purified by column chromatography (SiO_2/CH_2Cl_2, then SiO_2/19:1 hexane/EtOAc), giving 1.688 g of white solid (48%): mp = 73 °C; ^1H NMR ($CDCl_3$) δ 1.02 (s, 12 H, CH_3), 2.73 (s, 8 H, SCH_2), 2.86 (s, 8 H, SCH_2); IR (KBr) 2957, 2904, 1464, 1446, 1418, 1380, 1364, 1271, 1259, 1231, 1136, 912, 878, 844, 736, 690 cm^{-1}; EI-MS calcd for $C_{12}H_{24}S_4$ 324.1074, found 324.1070.

[2-Ni(ClO$_4$)$_2$](CH$_3$NO$_2$). To 10 mL of CH_3NO_2 in a 25-mL flask was added 183 mg (0.5 mmol) of $Ni(ClO_4)_2 \cdot (H_2O)_6$. Acetic anhydride (408 mg, 4 mmol) was added, and the mixture was stirred 10 min, by which time the solid had dissolved. Solid **2** (148 mg, 0.5 mmol) was added, whereupon a bright red color developed. The mixture was stirred 10 min, during which time the solid thioether dissolved. The red solution was added dropwise to 60 mL of stirred Et_2O, which led to the formation of an orange precipitate. The mixture was trituriated overnight, filtered, washed with 50 mL of Et_2O, and the resulting orange solid was dried on the vacuum line to give 272 mg (88%) of the desired complex. Anal. Calcd (found) for $C_{12}H_{24}S_4NiCl_2O_8 + CH_3NO_2$: C, 25.38 (25.41); H, 4.56 (4.42); Ni, 9.52 (9.54).

3-Ni(ClO$_4$)$_2$. To 5 mL of CH_3NO_2 in a 10-mL flask was added 147 mg (0.25 mmol) of $Ni(ClO_4)_2 \cdot (H_2O)_6$. Acetic anhydride (408 mg, 4 mmol) was added, and the mixture was stirred 10 min, by which time the solid had dissolved. Solid **3** (130 mg, 0.4 mmol) was added, causing a bright red color to develop. The mixture was stirred 10 min, by which time the solid thioether had dissolved. The red solution was added dropwise to 80 mL of stirred Et_2O, whereupon a red precipitate separated. The solid was trituriated overnight, filtered, washed with 25 mL of Et_2O, and dried on the vacuum line to give 214 mg (92%) of the desired complex. A sample was crystallized by vapor diffusion of 1,2-dichloroethane into a nitromethane solution of the complex. Anal. Calcd (found) for $C_{14}H_{28}S_4NiCl_2O_8 + C_2H_4Cl_2$: C, 28.21 (28.46); H, 4.74 (4.83); S, 18.83 (19.39); Ni, 8.58 (8.61).

Relative Binding Studies by ^1H NMR. Stock solutions of thioethers **1**–**3** and of Ni(II) in CH_3NO_2 were prepared, the latter by dissolving a weighed amount of $Ni(ClO_4)_2 \cdot (H_2O)_6$, combined with 10 equiv of acetic anhydride. NMR samples were prepared by mixing appropriate amounts of Ni and thioether stock solutions in a vial, removing the CH_3NO_2 under a stream of N_2, and drying the solid residue on a vacuum line. The residue was then redissolved in an appropriate amount of CD_3NO_2, which had been dried over $CaSO_4$ and distilled from a small amount of P_2O_5. The solution was briefly degassed with a N_2 stream and then transferred into a N_2-purged NMR tube. The final concentration was ~12.5 mM of each component. Several days standing at room temperature were required for these solutions to reach the equilibrium distribution of Ni(II) between macrocyclic chelators. Similar results were obtained when NMR samples were prepared from preformed nickel–thioether complexes. ^1H NMR spectra were recorded at 200 MHz. For integration, at least 16 scans were recorded, with a receiver delay of at least 2 s between scans.

X-ray Crystallography Procedure. Unless otherwise noted, the same general procedure was followed for determination of all solid-state structures by X-ray diffraction. Crystals were grown from ~2 mL of solution and were removed from solution prior to examination. The crystals were mounted on glass fibers and centered on the diffractometer. Initial lattice constants were found by location and centering of reflections from a rotation photo, and axial photos confirmed axial lengths and Laue symmetry. Accurate unit-cell constants were determined by centering of at least 15 high-angle reflections. Data were corrected for Lorenz/polarization effects.

Structure solution was accomplished with the SHEXTL direct methods facility; Fourier expansion from molecular fragments gave all non-hydrogen atoms, which were refined anisotropically. Hydrogen atoms, although visible in difference Fourier maps, were included in calculated positions with an overall temperature factor for all atoms. Methyl groups were refined as rigid bodies. Extinction correction and variable weighting were used for all data sets.

2: Long needles were obtained from vapor diffusion of MeOH into a $CHCl_3$ solution. Data were collected at low temperature and were corrected for absorption. Solution and refinement were uneventful.

3: Large, clear crystals, from which a piece was cut, were obtained by evaporation from a hexane solution. Absorption correction was attempted but significantly worsened fit, probably because of poor azimuthal scans. Solution was by direct methods. Because of the small size

(38) Nelson, E. R.; Maienthal, M.; Lane, L. A.; Benderly, A. A. *J. Am. Chem. Soc.* **1957**, *79*, 3467.
(39) Dawson, T. P. *J. Am. Chem. Soc.* **1947**, *69*, 1176.
(40) Buter, J.; Kellogg, R. M. *Org. Synth.* **1987**, *65*, 150.
(41) Eliel, E. L.; Rao, V. S.; Smith, S.; Hutchins, R. O. *J. Org. Chem.* **1975**, *40*, 524.

of the asymmetric unit, there was significant correlation in the least-squares refinement, and damping was required for initial stages of refinement.

2-Ni: Red plates were obtained from vapor diffusion of $ClCH_2CH_2Cl$ into a CH_3NO_2 solution. CH_3NO_2 was found in the difference Fourier map; anisotropic refinement was successful. Large thermal anisotropy was evident in the counterions, but was not further modeled.

3-Ni: Large red prisms were grown by vapor diffusion of $ClCH_2CH_2Cl$ into a CH_3NO_2 solution. A difference peak was ascribed to $ClCH_2CH_2Cl$; the solvent molecule resides on an inversion center and was successfully refined with anisotropic thermal motion. Much disorder, interpreted as rotation about a Cl-O bond of a perchlorate anion, was evident; the remaining three oxygens were refined as disordered pairs, each with half occupancy and isotropic thermal motion constrained to 0.03. Residual electron density was near the perchlorate.

Acknowledgment. S.H.G. thanks the Searle Scholars Program and the American Cancer Society (Junior Faculty Research Award) for partial support. J.M.D. thanks the Graduate School of the University of Wisconsin—Madison for a fellowship. S.R.C. acknowledges support from the Petroleum Research Fund, administered by the American Chemical Society. S.H.G. thanks Tim Clark (Visiting Professor of Chemistry, University of Wisconsin—Madison, Spring 1991) for helpful discussions on computational issues.

Spectroscopic and Theoretical Studies of an End-On Peroxide-Bridged Coupled Binuclear Copper(II) Model Complex of Relevance to the Active Sites in Hemocyanin and Tyrosinase

Michael J. Baldwin,[†] Paul K. Ross,[†] James E. Pate,[†,‡] Zoltán Tyeklár,[§] Kenneth D. Karlin,[§] and Edward I. Solomon*,[†]

Contribution from the Department of Chemistry, Stanford University, Stanford, California 94305, Department of Chemistry, The Johns Hopkins University, Baltimore, Maryland 21218, and Dow Chemical Company, Central Research, Advanced Polymeric Systems Laboratory, Midland, Michigan 48674. *Received April 25, 1991*

Abstract: Spectroscopic studies have been combined with broken-symmetry SCF-Xα-SW calculations to determine the vibrational and electronic structure of peroxide–copper bonding in the end-on trans μ-1,2 peroxide-bridged copper dimer, $[\{Cu(TMPA)\}_2(O_2)]^{2+}$. This study provides a detailed understanding of the electronic structure generally associated with an end-on peroxide-bridging mode and additionally shows important dimer interactions which are not present in the copper–peroxide monomer. The Xα calculations show that the electronic structure is dominated by the interaction of the peroxide π^*_σ orbital with the half-occupied copper d_{z^2} orbitals. This copper–peroxide bonding is probed experimentally by a peroxide-to-copper charge-transfer spectrum which contains three transitions at 615 (ϵ = 5800 M^{-1} cm^{-1}), 524 (ϵ = 11 300 M^{-1} cm^{-1}), and 435 nm (ϵ = 1700 M^{-1} cm^{-1}) assigned as the electric dipole allowed singlet transitions from π^*_ν and π^*_σ (the HOMO orbitals of peroxide) and the spin-forbidden triplet from π^*_ν, respectively. The differences between the observed and calculated transition energies, which are present in the dimer but not the monomer, are shown to arise from excited-state splittings which derive from excitation transfer in the dimer and from excited-state exchange interactions much larger than those in the dimer ground state [$-2J_{es}(\pi^*_\nu) \approx 7600$ cm^{-1}]. The resonance Raman spectra show two enhanced vibrations which shift upon isotopic substitution of $^{16}O_2$ by $^{18}O_2$ at 832 (788 cm^{-1} with $^{18}O_2$) and 561 cm^{-1} (535 cm^{-1} with $^{18}O_2$). They are assigned as the intraperoxide stretch and the symmetric copper–oxygen stretch, respectively. A normal-coordinate analysis has been performed using these vibrational data to compare this trans μ-1,2 dimer to a previously studied monomer. This analysis shows that the O–O bond force constant, k_{O-O}, increases upon going from the monomer to the dimer due to increased donation of electron density from the antibonding π^*_σ orbital to the second copper in the dimer. The resonance enhancement of the intraperoxide stretch is similar to that of the monomer; however, the enhancement behavior of the copper–oxygen stretch is significantly different from that in the monomer, showing enhancement only from the π^*_ν transitions. This enhancement behavior is discussed with respect to excited-state distortions of the dimer which can be very different from the monomer depending on the extent of delocalization (i.e. electron coupling) of the charge-transfer excitation over the two halves of the dimer.

Introduction

The electronic, vibrational, and chemical properties of copper–peroxide bonding have long been of interest due to the importance of copper–peroxide complexes in reversible oxygen binding and oxidation and oxygenation catalysis, especially in such biological systems as hemocyanin,[1] tyrosinase,[2] and the multicopper oxidases.[3] Several different binding modes of peroxide to copper(II) are known. An end-on bound monomer[4] (structure A in Scheme I), $[Cu_2(XYL-O-)(O_2)]^+$, was studied previously in solution but could not be crystallized. Complexes with a binding mode like that of structure B in Scheme I are also known,[5] and a μ-1,1 acylperoxo complex of this type has been structurally characterized.[6] While the cis μ-1,2 structure C of Scheme I is

* Author to whom correspondence should be directed.
† Stanford University.
§ Johns Hopkins University.
‡ Dow Chemical Company.

(1) (a) Solomon, E. I.; Penfield, K. W.; Wilcox, D. E. *Structure and Bonding (Berlin)* **1983**, *53*, 1–57. (b) Solomon, E. I. *Pure Appl. Chem.* **1983**, *55*, 1069–1088. (c) Solomon, E. I. In *Copper Proteins*; Spiro, T. G., Ed.; Wiley: New York, 1981; pp 41–108.

(2) Lerch, K. *Metal Ions Biol. Syst.* **1981**, *13*, 143–186.

(3) (a) Cole, J. L.; Tan, G. O.; Yang, E. K.; Hodgson, K. O.; Solomon, E. I. *J. Am. Chem. Soc.* **1990**, *112*, 2243–2249. (b) Andreasson, L. E.; Branden, R.; Reinhammer, B. *Biochim. Biophys. Acta* **1976**, *438*, 370–379.

(4) (a) Pate, J. E.; Cruse, R. W.; Karlin, K. D.; Solomon, E. I. *J. Am. Chem. Soc.* **1987**, *109*, 2624–2630. (b) In this paper the term "monomer" refers to peroxide bound to a single copper ion; the term "dimer" refers to peroxide bridging a pair of copper ions and mediating interactions between those copper ions.

(5) Karlin, K. D.; Cruse, R. W.; Gultneh, Y. *J. Chem. Soc., Chem. Commun.* **1987**, 599–600.

0002-7863/91/1513-8671$02.50/0